

150. Two-Dimensional NMR Studies of Polyene Systems. I. All-*trans*-Retinal

by Jacques Wernly and Jürgen Lauterwein

Institut de chimie organique de l'Université, 2, rue de la Barre, CH-1005 Lausanne

(3. III. 83)

Summary

Two-dimensional (2-D) NMR results are presented for all-*trans*-retinal. 2-D *J*-resolved ^1H -NMR separated the multiplets of the olefinic protons and accurately determined their chemical shifts. 2-D shift-correlated ^1H -NMR gave the connectivities between scalar coupled protons. From the observed H,H long-range couplings the assignment of the methyl resonances was possible. 2-D *J*-resolved ^{13}C -NMR separated overlapping C,H-multiplets and allowed analysis of the C,H long-range couplings. 2-D shift-correlated ^{13}C -NMR related each directly bonded C,H-pair in this molecule. The potential of 2-D NMR in resolving and identifying individual resonances in polyene spectra is discussed.

Introduction. – Two-dimensional NMR (2-D NMR), after having been pioneered in Oxford [1–3] and in Zürich [4–6], seems to be on the way to routine application in chemistry laboratories. This is mainly due to the progress in NMR spectrometer and data-system capabilities [7]. In the last few years successful applications of 2-D NMR have been reported on amino acids [8], peptides [9] [10], proteins [11–13], steroids [14], oligosaccharides [15] [16] and polynucleotides [17] [18]. To gain a detailed understanding of the conformation of retinoids, carotenoids and polyene antibiotics in various biologically interesting environments [19] [20] we became interested in applying 2-D NMR methods to these polyene systems. For their structural analysis it is of utmost importance to know the correct assignments of the resonances in the ^1H - and ^{13}C -NMR spectra. This often turns out to be a difficult task in conventional 1-D NMR spectroscopy, since even at the highest magnetic fields available, the region of the olefinic H- and C-resonances is very crowded [21–23]. The difficulties increase with increasing chain length of the polyene chain, or when the analysis of a mixture of isomers is required. In the present work we have chosen all-*trans*-retinal (ATR, **1**) as a model substance to perform the most common 2-D *J*-resolved and shift-correlated ^1H - and ^{13}C -NMR experiments [3]. Since the 1-D NMR spectra of **1** have been analyzed and the assignments of the ^1H - [24–26] and ^{13}C -resonances [27–29] are well-established, this compound should allow us to discuss the potential advantages and limitations

of the various 2-D NMR techniques with respect to our future study of more complex polyene systems.

Experimental. - All-*trans*-retinal was purchased from *Fluka*. Solutions were made up in C^2HCl_3 and protected from light. Solution concentrations were 0.03 M for 1H -NMR (5-mm sample tubes) and 0.2 M for ^{13}C -NMR (10-mm sample tubes). The spectra were obtained at 30° on a *Bruker-WH-360* instrument operating under the control of an *Aspect-2000* pulse generator and data system. All chemical shifts are in ppm relative to internal TMS. The 90° pulse length at 360 MHz (1H) was 7 μ sec using the 1H -probehead and 36 μ sec through the decoupler coil of the ^{13}C -probehead; at 90.5 MHz (^{13}C) it was 13.5 μ sec. Quadrature detection was employed exclusively. Spectra simulation was performed by the PANIC program on the *Aspect-2000*. All 2-D spectra were obtained by the FTQNMNMR program version 810515 and were processed by the FT2DNMR program version 820701. The latter allowed absolute-value data display only. Details for each 2-D experiment are described below.

2-D J-Resolved 1H -NMR. The pulse sequence 90°- $t_1/2$ -180°- $t_1/2$ -FID(t_2) was used. t_1 is the variable time domain prior to detection (evolution period) and t_2 is the time domain of the FID (detection period). A 16-phase cycle [30] was used to cancel pulse errors. The number of sample data points was $X_1=256$ in t_1 and $X_2=4 K$ in t_2 . Zero-filling to $N_1=512$ data points was used in t_1 . The spectral width was ± 32 Hz in f_1 and 4 kHz in f_2 . Sixteen transients were collected for each t_1 increment ($\Delta t_1/2=7.8$ msec). The recycle delay was 4 sec. The time for data acquisition was approx. 7 h. The $512 \times 4 K$ transformation with 45° tilt required approx. 2.5 h.

2-D Shift-correlated 1H -NMR. The pulse sequence 90°- $t_1/2$ -90°- $t_1/2$ -FID(t_2) was used (SECSY spectrum). The same phase cycle as above was applied (negative-type peak selection [31]). The

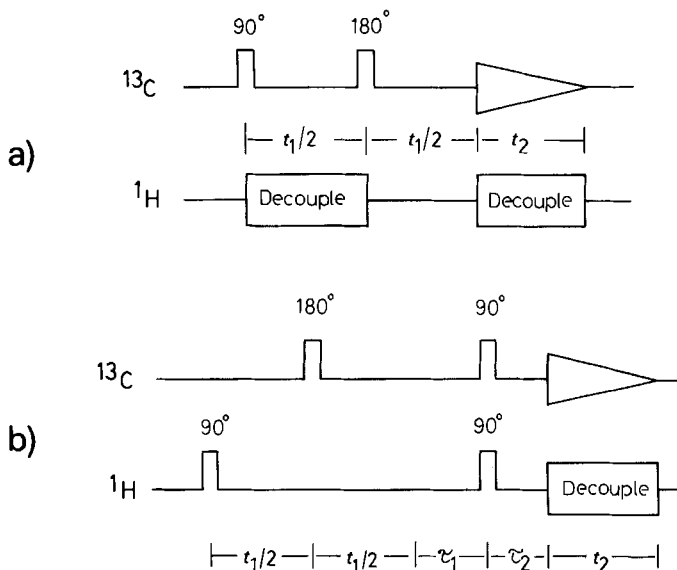


Fig. 1. Pulse sequences used in the 2-D ^{13}C -NMR experiments.

a) *J-Resolved spectroscopy* (gated-decoupler mode): the proton-coupled precession of the ^{13}C spins is allowed during one half of the evolution period t_1 and decoupled precession during the other half.
 b) *Shift-correlated spectroscopy*: the magnetization transfer from 1H to ^{13}C is accomplished by the 90° pulses, while 1H , ^{13}C -splittings are suppressed by the ^{13}C 180° pulse in the t_1 dimension, and by the use of proton noise decoupling in the t_2 dimension. τ_1 is the time development for polarization, optimum $\tau_1=(2J)^{-1}$ for all $^{13}CH_n$ -systems ($n=1,2,3$). τ_2 is the refocusing time for antiphase signals, optimum $\tau_2=(2J)^{-1}$ for ^{13}CH selection, approx. $(4J)^{-1}$ as a compromise for various $^{13}CH_n$ -multiplicities.

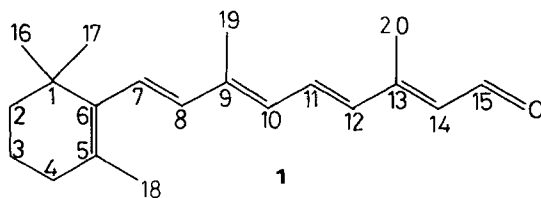
following parameters have been used: $X_1=256$, $X_2=2 K$; multiplication in both time domains with a sine-bell function [32]; zero-filling to $N_1=1 K$; spectral width ± 1 kHz in f_1 , 4 kHz in f_2 ; number of transients for each t_1 increment $NS=16$ ($\Delta t_1/2=0.25$ msec); recycle delay 4 sec. Acquisition approx. 5 h, $1 K \times 2 K$ transformation approx. 2 h.

2-D J-Resolved ^{13}C -NMR. The pulse sequence of *Figure 1a* was used ('gated decoupling' experiment). Proton-noise decoupling was turned off during the second $t_1/2$ period. Phase cycling as in [30]. Parameter settings: $X_1=128$, $X_2=2 K$; no window functions; zero-filling to $N_1=256$ and $N_2=4 K$; spectral width ± 78 Hz in f_1 , 20 kHz in f_2 ; $NS=96$; $\Delta t_1/2=3.2$ msec; recycle delay 4 sec. Data acquisition approx. 15 h, $256 \times 4 K$ transformation approx. 1 h.

2-D Shift-correlated ^{13}C -NMR. The pulse sequence used for obtaining $^1H, ^{13}C$ chemical-shift correlated spectra is shown in *Figure 1b*. The magnetization transfer was made via the $^1J(C,H)$ couplings. τ_1 for polarization and τ_2 for ^{13}CH selection was chosen to be equal to $(2J)^{-1} \approx 3.2$ msec. The phase program [33] allowed quadrature detection in f_1 . Other parameters: $X_1=128$, $X_2=2 K$; sine-bell in t_1 and t_2 ; zero-filling to $N_1=512$; spectral width ± 380 Hz in f_1 , 1.6 kHz in f_2 (chosen such as to detect only the olefinic H- and C-atoms); $NS=64$; recycle delay 4 sec; $\Delta t_1/2=0.66$ msec. Acquisition approx. 9 h, $512 \times 2 K$ transformation approx. 1 h.

Results. – 1. *2-D J-Resolved 1H -NMR spectroscopy.* This technique [5] [6] was used to separate the overlapping multiplets of **1** and to obtain a homonuclear decoupled 'chemical-shift spectrum'. The projection along the f_2 or chemical-shift axis is shown in *Figure 2* for the olefinic protons of **1**. All individual chemical shifts could be resolved. Since the chemical-shift difference of H-C(8) and H-C(10) was only 0.2 ppm (7 Hz at 360 MHz), the digital resolution in f_2 -direction was adopted to 2 Hz/point. The intensities of the projected lines turned out to be very different for the various olefinic protons (*Fig. 2*). No sine-bell window function was applied in the t_2 -domain to avoid the near suppression of the low-intensity signals of H-C(7) and H-C(10). It is important to note that an extra peak appeared midway between the projections of H-C(7) and H-C(8) (asterisk in *Fig. 2*). It is the result [8] [35] [36] of the second-order character of this spin system (*AB*-effect, $J/\Delta\delta \approx 0.3$).

The *J*-cross-sections [6] gave well-analyzable multiplet patterns. In *Figure 3* we present only those of H-C(8) and H-C(11). Comparing the multiplets of *Figure 3a* with the 1-D spectrum in *Figure 2a* a similar resolution was obtained, although the absolute-value representation [6] was applied. Application of a window function in t_1 -direction allowed to resolve several long-range coupling constants. Thus, in *Figure 3b* the doublet character of each line originates [26] from the couplings $^4J(H-C(8), H-C(10))$ and $^5J(H-C(11), H-C(14))$, respectively. The *Table* collects the apparent coupling constants of H-C(8) and H-C(11) measured after the application of various window functions in t_1 and compares them with the values obtained earlier from 1-D analysis by spin decoupling and spectrum simulation [26]. The coupling constants measured from the *J*-cross-sections depend clearly



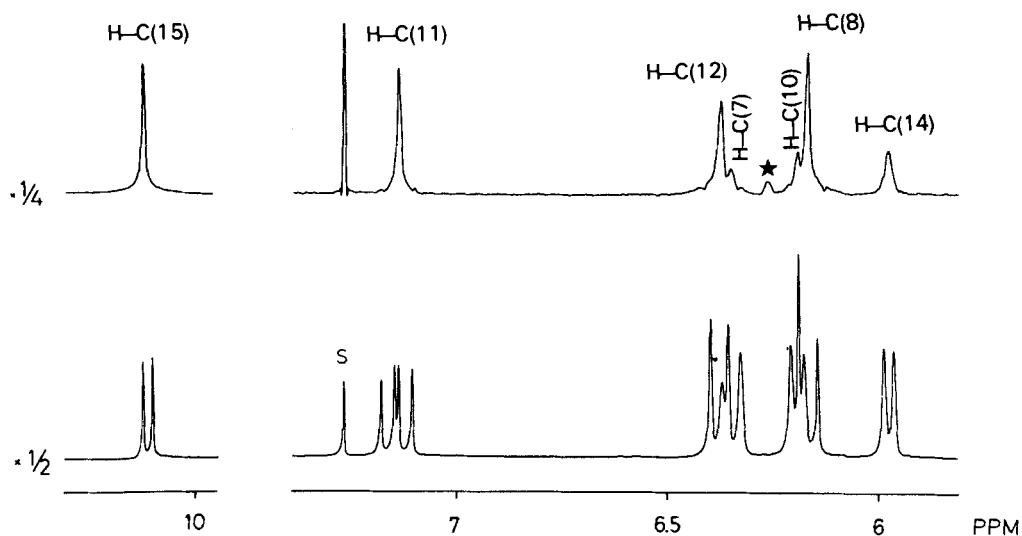


Fig. 2. 2-D J-Resolved $^1\text{H-NMR}$ (360 MHz) of all-trans-retinal in C^2HCl_3 . A normal 1-D $^1\text{H-NMR}$ of the olefinic protons (lower trace) is compared with the 'homonuclear decoupled' spectrum obtained from the projection of the 2-D spectrum on the f_2 (chemical shift) axis. No window functions were applied in both time domains. The resonance assignments are in agreement with previous work [26] [34]. * indicates extra peak from strong coupling between H-C(7) and H-C(8). The resonance of H-C(15) is shown at reduced amplitude ($\frac{1}{4}$ and $\frac{1}{2}$, resp.). The peak marked s is from residual C^1HCl_3 .

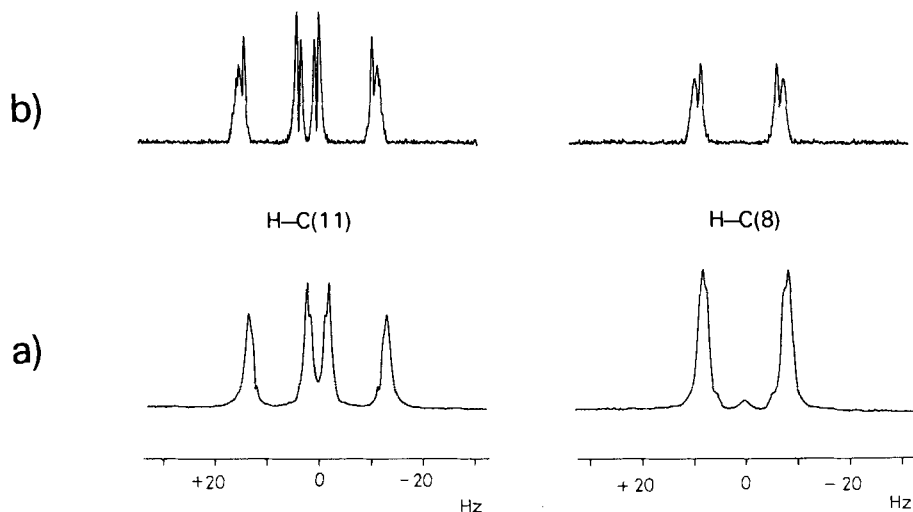


Fig. 3. Cross-sections parallel to the f_1 (J) axis for the protons H-C(8) and H-C(11) of all-trans-retinal. Experimental conditions as in Fig. 2, except for the window functions applied: spectra a) without function, spectra b) with sine-bell functions in both t_1 and t_2 . The multiplets have undergone symmetrization [37]. Digital resolution in J -direction is 0.12 Hz/point.

upon the type of window function chosen (*Table*). The error is largest for the small coupling constants, and their magnitude tends to increase with increasing 'strength' of the function. Thus, for ${}^4J(\text{H}-\text{C}(8), \text{H}-\text{C}(10))$ an apparent increase of more than 100% was observed after application of the sine-bell function. This confirmed that the absolute-value representation induces errors in the line positions when the resonances are partially overlapping [38].

2. *2-D Shift-correlated ${}^1\text{H-NMR}$ spectroscopy.* Of the various methods to obtain J -connectivities we have chosen the spin-echo correlated spectroscopy (SECSY) [39] [40]. The SECSY spectrum of **1** is shown as a stacked plot (*Fig. 4*) and in a contour-plot representation (*Fig. 5*). In f_1 -direction the differences between the chemical shifts of the coupled protons are represented. Each proton gives a response along the principal axis at $\Delta\delta=0$, together with one off-axis response for each resonance with which it shares a scalar coupling. The effective sweep width in f_1 was selected as the chemical shift difference between the aliphatic and olefinic regions of **1** (approx. ± 3 ppm, assuming negligible long-range couplings for $\text{H}-\text{C}(15)$). In *Figure 5* a single off-axis response was observed for $\text{H}-\text{C}(15)$ at half the chemical shift difference between $\text{H}-\text{C}(15)$ and $\text{H}-\text{C}(14)$. An equivalent response was obtained for $\text{H}-\text{C}(14)$ on the other side of the principal axis. $\text{H}-\text{C}(11)$ has two off-axis responses which correlated with $\text{H}-\text{C}(10)$ and $\text{H}-\text{C}(12)$. Correlation between the multiplets worked out also in the strongly coupled system of $\text{H}-\text{C}(7)$ and $\text{H}-\text{C}(8)$. All the connectivities from the vicinal couplings of the olefinic protons could be clearly seen, as well as those of the CH_2 -protons in the β -ionone ring. To avoid that the off-axis responses located close to the principal axis are obscured by the direct responses (*e.g.* in the case of $\text{H}-\text{C}(7)$ and $\text{H}-\text{C}(8)$), an efficient resolution-enhancement in f_1 -direction was applied. Besides the correlation of the olefinic protons by their vicinal couplings (no geminal J 's exist in the polyene chain of **1**) we could detect (*Fig. 5*) four off-axis responses which derive from the couplings corresponding to ${}^4J(\text{H}-\text{C}(10), \text{H}_3\text{C}(19))$, ${}^4J(\text{H}-\text{C}(14), \text{H}_3\text{C}(20))$, ${}^5J(\text{H}-\text{C}(7), \text{H}_3\text{C}(18))$, and ${}^5J(\text{H}-\text{C}(7), \text{H}_2\text{C}(4))$. These long-range J 's were easy to distinguish from the vicinal J 's by the much smaller intensity of their off-axis

Table. H, H -Coupling constants $J(\text{Hz})$ for $\text{H}-\text{C}(8)$ and $\text{H}-\text{C}(11)$ of all-trans-retinal^a) measured from the 2-D J -cross-sections after application of different window functions

Couplings	2-D NMR					1-D NMR	
	Window functions						
	in t_1 :	^{b)}	^{c)}	^{d)}	^{e)}		^{f)}
in t_2 :	^{b)}	^{c)}	^{c)}	^{c)}	^{c)}		
$\text{H}-\text{C}(8), \text{H}-\text{C}(7)$	15.6	15.9	15.8	16.0	16.0	16.2	
$\text{H}-\text{C}(8), \text{H}-\text{C}(10)$	^{b)}	-0.5	-0.6	-1.2	-1.4	-0.6	
$\text{H}-\text{C}(11), \text{H}-\text{C}(12)$	14.7	14.7	14.7	14.6	14.4	15.0	
$\text{H}-\text{C}(11), \text{H}-\text{C}(10)$	11.3	11.3	11.3	11.2	11.0	11.5	
$\text{H}-\text{C}(11), \text{H}-\text{C}(14)$	^{b)}	0.6	0.8	1.0	0.8	0.55	

^{a)} 0.03M in C_2HCl_3 , $T=30^\circ$. ^{b)} No function. ^{c)} Sine-bell shifted $\pi/2$. ^{d)} Sine-bell shifted $\pi/6$. ^{e)} Sine-bell. ^{f)} Squared sine-bell. ^{g)} Values taken from [26]; for observation of the long-range couplings 3 $\text{H}-\text{C}(19)$ was decoupled. ^{h)} Splitting not sufficiently resolved.

peaks (Fig. 4). According to the 1-D analysis of Karplus *et al.* [25] [26] these are the largest long-range coupling constants found in **1** with values between 0.8 and 1.5 Hz. Coupling constants < 0.8 Hz, although existing in the $^1\text{H-NMR}$ of **1** [26], could not be detected under the present experimental conditions (see *Discussion*).

3. 2-D *J*-Resolved $^{13}\text{C-NMR}$ spectroscopy. The 1-D ^1H -coupled $^{13}\text{C-NMR}$ spectrum of **1** shows considerable overlapping of the multiplets from the olefinic C-atoms, in particular for C(7), C(10) and C(14) (Fig. 6c). 2-D *J*-resolved spectroscopy [41] [42] allowed the separation of C,H-coupling information from chemical-shift information. Of the three basic techniques available we have performed the ‘gated-decoupling’ spin-echo sequence (Fig. 1a). The *J*-resolved contour plot of the olefinic C-region of **1** is represented in Fig. 6a. Apart from an easy recognition of the C-multiplicities, the C,H-long-range couplings could be well-resolved (digital resolution in f_1 was 0.6 Hz/point). The coupling pattern in the *J*-cross-sections allowed an unambiguous assignment of the resonances from C(7), C(10) and C(14) (Fig. 7): C(14) reveals a coupling of 25.6 Hz which is characteristic [43] for the 2J with the aldehyde proton H-C(15); C(7) demonstrates a second-order pattern which is expected due to its coupling with the *AB*-system of H-C(7) and H-C(8). From simulation (Fig. 7) the following parameters were obtained: $^3J(\text{H-C}(7), \text{H-C}(8)) = 15.9$ Hz, $^1J(\text{C}(7), \text{H-C}(7)) = 155.2$ Hz, $^2J(\text{C}(7), \text{H-C}(8)) = -3.0$ Hz; chemical shift difference between H-C(7) and H-C(8) = 63 Hz. Finally, C(10) can be assigned by elimination, if the assignment of the residual olefinic C-atoms is known [27]. Although in the 2-D gated-decoupling experiment all *J*-values are scaled as 1/2 their actual magnitude [42], the resolution of the multiplets appeared comparable to that obtained in the 1-D spectrum after resolution enhancement.

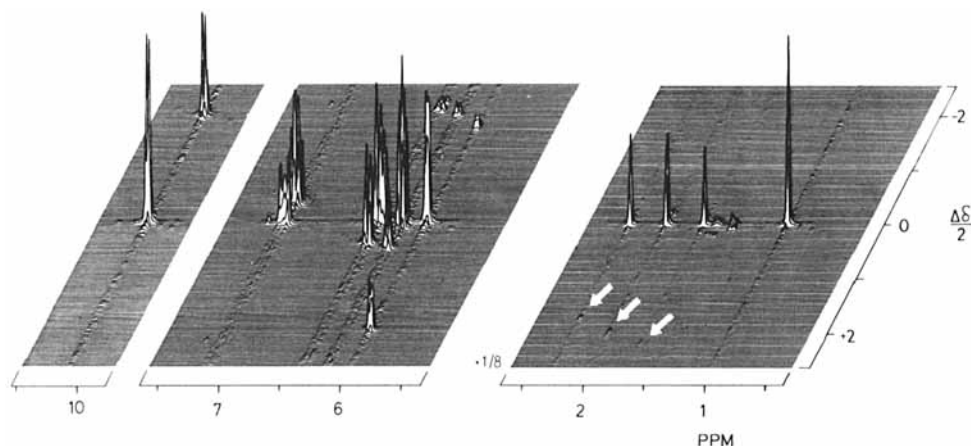


Fig. 4. 2-D Shift-correlated $^1\text{H-NMR}$ (360 MHz) of all-trans-retinal in C_2HCl_3 , stacked plot of a SECSY spectrum. The shift axis is horizontal. The low-frequency region is shown at $1/8$ the intensity of the olefinic region. Arrows indicate the off-axis responses from long-range couplings of the CH_3 -groups with the olefinic protons.

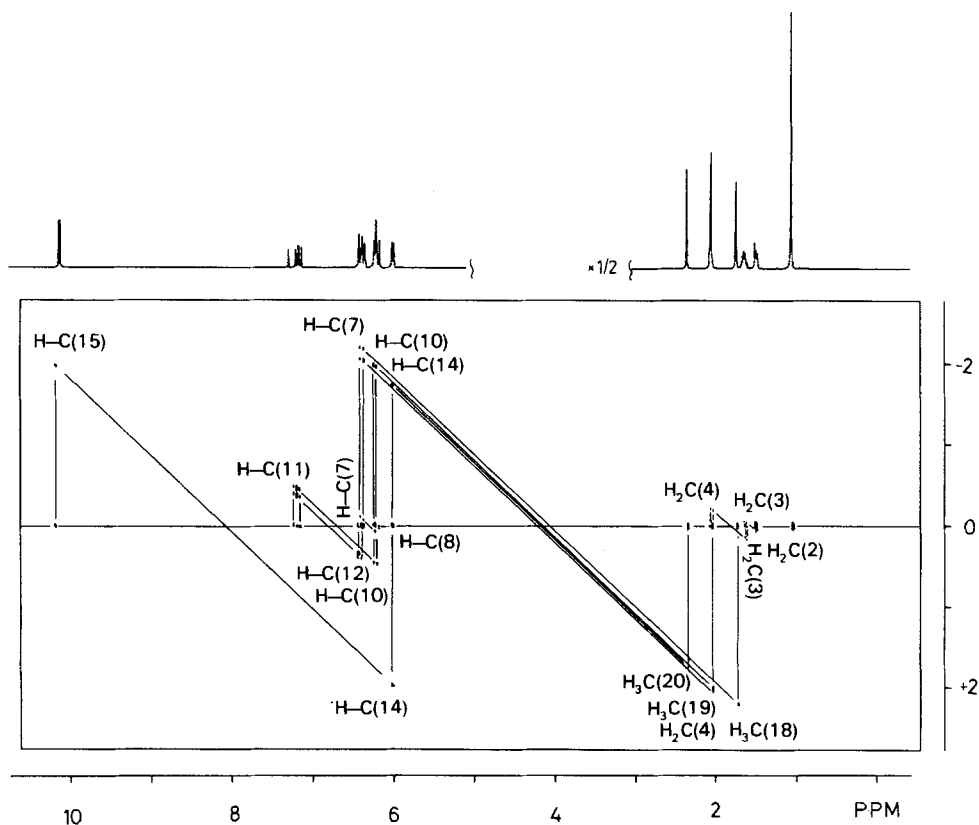


Fig. 5. 2-D Shift-correlated $^1\text{H-NMR}$ (360 MHz) of all-trans-retinal in C^2HCl_3 , contour-plot representation of the SECSY spectrum of Fig. 4. The contours were taken at different levels to give maximum resolution. All observed correlations are drawn. A 1-D spectrum is plotted on top (two-fold amplification of the olefinic region).

4. 2-D Shift-correlated $^{13}\text{C-NMR}$ spectroscopy. This technique (pulse sequence in Fig. 1b) allows a mapping of the $^{13}\text{C-NMR}$ chemical shifts against the $^1\text{H-NMR}$ chemical shifts [3]. Magnetization transfer via the olefinic $^1J(\text{C},\text{H})$ couplings in **1** resulted in the contour plot of Figure 8. The time delays τ_1 and τ_2 (Fig. 1b) were chosen to be equal and were adjusted to give maximum polarization for the average $^1J(\text{C},\text{H})$ -value of 155 Hz. 'Tuning' for 1J was rather easy since the couplings in the polyene chain of **1** differ very little (see Fig. 6a). Knowing the assignments in the $^1\text{H-NMR}$ spectrum of **1**, all resonances of the protonated C-atoms in the polyene chain could be assigned independently (Fig. 8). Assignment of C(7), C(10) and C(14) was possible even with poor resolution in f_1 since the corresponding proton resonances were well-separated. When the proton chemical shifts were similar, e.g. for H-C(8) and H-C(12), the corresponding C-atoms C(8) and C(12) could be distinguished by looking at the details of the cross-sections through each ^{13}C -

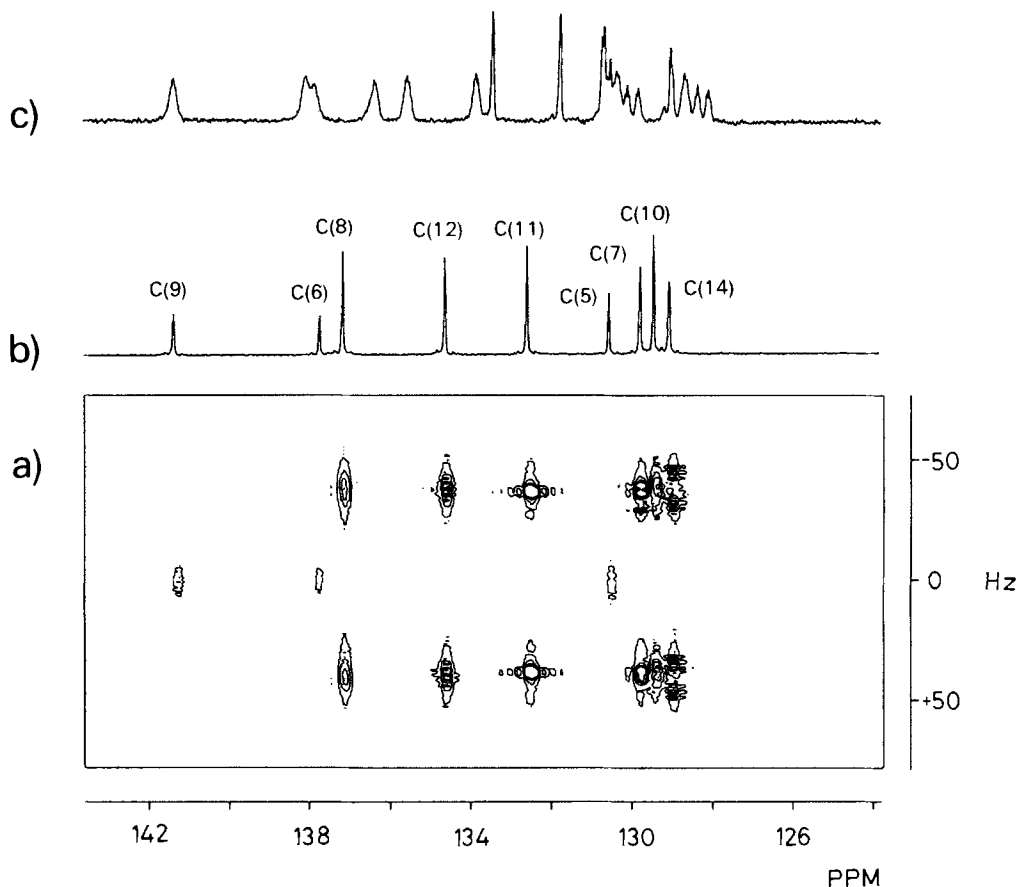


Fig. 6. 2-D *J*-Resolved ^{13}C -NMR (90.5 MHz) of all-trans-retinal in C^2HCl_3 , via the gated-decoupling technique. a) Contour plot of the olefinic C-atoms (C(13) at 155.2 ppm and C(15) at 191.2 ppm are omitted). b) 1-D Proton-noise decoupled ^{13}C -NMR. Resonance assignments are in agreement with previous work [27] [34]. c) 1-D Proton-coupled ^{13}C -NMR with strong overlapping of the resonances from C(5), C(7), C(10) and C(14).

chemical shift. With sufficient resolution in f_1 (1.5 Hz/point) the vicinal proton couplings could be resolved, and the assignment of the C-atoms was possible because of the difference in ${}^3J(\text{H}-\text{C}(8), \text{H}-\text{C}(7)) \approx 16$ Hz and ${}^3J(\text{H}-\text{C}(10), \text{H}-\text{C}(11)) \approx 11$ Hz [34]. At the level of the contour plot chosen, no complex polarization transfer from the strong *AB*-effects of H-C(7) and H-C(8) could be observed.

Discussion. – Recently 2-D *J*-resolved ^1H -NMR spectra of two carotenoids have been reported by Englert [44], and the potential of this technique to separate different multiplets in the strongly overlapping olefinic regions of these compounds was acknowledged. In **1** we meet spin systems which range from strong to weak coupling. In some cases the *J*-cross-sections of the olefinic protons allow their individual identification from the vicinal coupling pattern (e.g. the doublet of

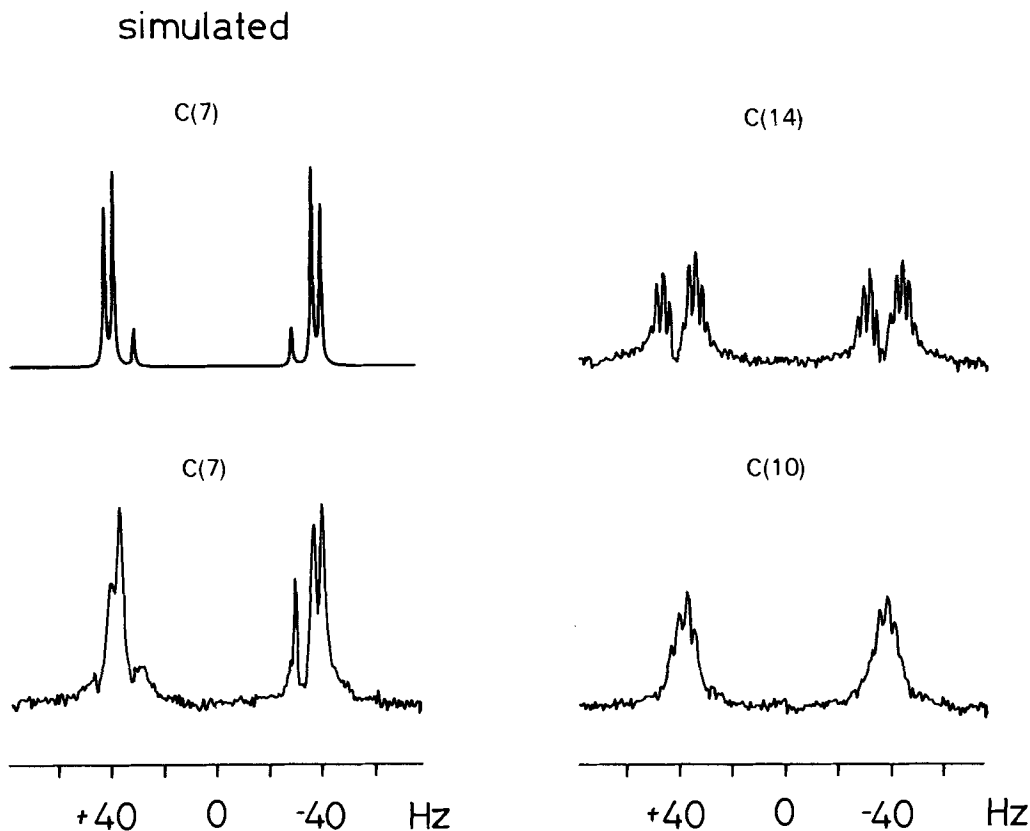


Fig. 7. *J*-Cross-sections for C(7), C(10) and C(14) of all-trans-retinal as taken from the 2-D matrix of Fig. 6a (no window functions applied). Note that the *J*'s are scaled by $\frac{1}{2}$. The simulation of the multiplet of C(7) is shown (*X*-part of an *ABX*-spectrum).

doublets of H–C(11)). However, since the multiplets are not ‘connected’ by a spin-spin coupling or by a nuclear *Overhauser* information, the assignments of the olefinic protons cannot be rigorously made from *J*-resolved NMR. Furthermore, the coupling constants determined from the *J*-multiplets (*Table*) have to be considered with precaution when the absolute-value mode representation is chosen and, at the same time, window functions are applied. In particular the magnitude of the long-range couplings appears strongly modified in this way (*Table*). Since the apparent coupling constants depend on the ‘strength’ of the window function, we see that the better resolution obtained from 2-D *J*-resolved spectra is only fictitious. Having obtained the 2-D chemical-shift and coupling parameters it is by all means indispensable to perform a simulation of the 1-D spectrum using an iterative program. An analysis of phase-sensitive spectra [45] should be envisaged in the future.

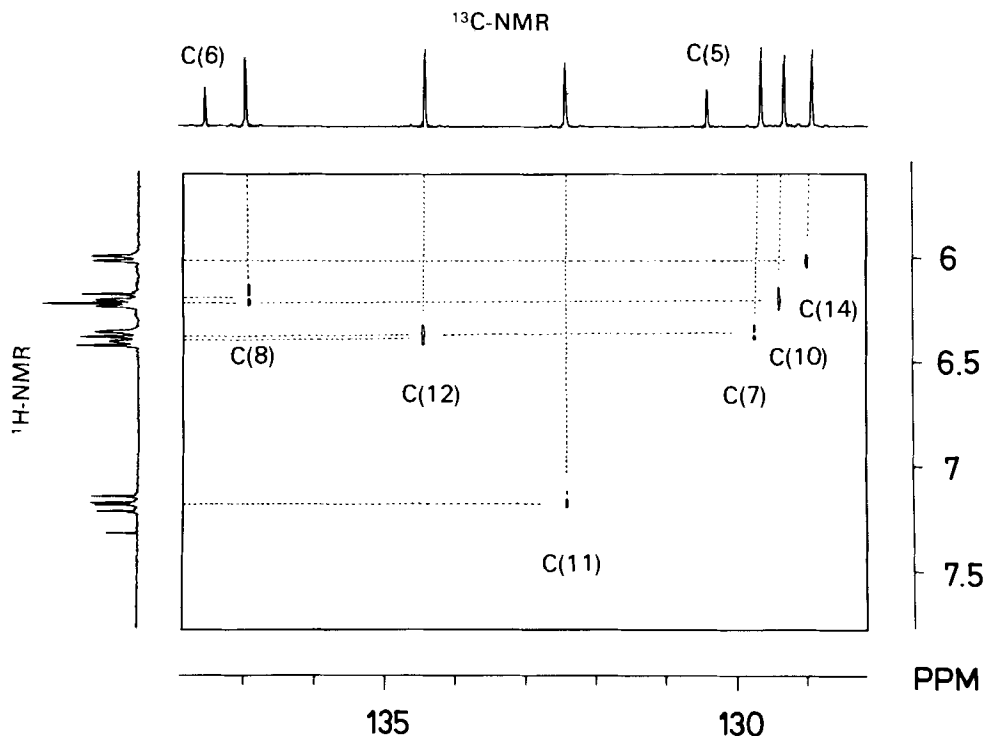


Fig. 8. 2-D Shift-Correlated $^{13}\text{C-NMR}$ (90.5 MHz) of *all-trans-retinal* in C^2HCl_3 . The correlation was made via the $^1\text{J}(\text{C},\text{H})$ couplings. Only the low frequency part of the olefinic-C-resonances is shown. Each peak in the contour plot corresponds to one CH-group (quaternary C-atoms do not show up). On the left: 1-D $^1\text{H-NMR}$ spectrum. On top: 1-D $^{13}\text{C-NMR}$ spectrum.

To obtain the chemical shifts of the olefinic protons of **1** from the projection of the J -multiplets, a sufficient digital resolution in f_2 is necessary. Apart from the aldehyde proton H-C(15) all six olefinic protons occur within a shift range of 1.2 ppm, and this situation will become worse when more complex polyene systems are investigated, e.g. ethyl β -apo-8'-carotenoate has 11 protons within 0.5 ppm [21] (2-D analysis to be published). Two possible problems are indicated by the present studies for the 2-D J -resolved spectroscopy of polyene systems: *i*. the intensities of the projection-lines are very different for the various olefinic protons (Fig. 2), an effect which is not understood at present, and there is great risk to lose some peaks when resolution enhancement functions are applied in the t_2 -domain; *ii*. since the ideal separation of the two frequency axes is possible only for the case of weakly coupled systems [36], any AB -effect will introduce extra peaks in the projection spectrum (Fig. 2). The real signals can be distinguished from the second-order artefacts by analysis of the cross-sections [35].

The three other 2-D experiments reported here were applied for the first time to polyene systems such as **1**. The utility of the SECSY spectrum is immediately

evident from *Figure 4* in which the chemical shifts of the olefinic protons of **1** are clearly correlated by their vicinal couplings, and this even in the strong *AB*-case of H–C(7), H–C(8). One might regret the limit of 0.8 Hz found for the detection of long-range couplings. To observe smaller long-range effects not resolvable in the 1-D spectrum [26], the evolution period t_1 should be increased since magnetization transfer between spins grows according to $\sin(\pi J t_1)$ [3]. When the assignment of the olefinic protons has been established, e.g. by a combination of 1-D and 2-D *J*-resolved and shift-correlated methods, an unequivocal assignment of the CH₃-resonances can be obtained from their long-range couplings with neighbouring olefinic protons (*Fig. 4*).

The 2-D *J*-resolved ¹³C-NMR spectrum of **1** (*Fig. 5*) demonstrates how efficient overlapping CH-multiplets can be separated. It remains to be examined if the resolution obtained by the 2-D gated-decoupling technique can be improved over that in the 1-D experiment. Although effects of field inhomogeneity are cancelled by the spin-echo sequence (*Fig. 1a*), resolution of the multiplets is limited since the *J*-values are only half their actual magnitude. This may be improved by either the spin-flip [42] or the INEPT [46] technique. For the analysis of long-range C, H-couplings in **1** one should also consider the spin-flip sequence using selective 180° proton pulses [47].

The fourth experiment performed with **1** correlates the ¹³C and ¹H chemical shifts *via* the ¹*J*(C, H) couplings (*Fig. 7*). Knowing the assignments of the proton resonances, those of the resonances from the protonated C-atoms followed without ambiguity. Earlier assignments, although in accordance with the present results, have been made by a laborious combination of ¹H off-resonance decoupling experiments, spin-lattice relaxation time measurements and lanthanide shift titrations [27–29]. Assignment of the resonances from C(7), C(10) and C(14), the most delicate because of their similar chemical shifts and their variation with temperature [48], could be made by 2-D shift correlation even under conditions of limited data matrix and experimental time. For the case of low resolution in f_1 it might be convenient to eliminate the ¹H multiplet structure for better correlation. Parabolic interpolation [49] appears to be useful if the ¹H-multiplet is symmetrical about the chemical shift frequency. It remains to be shown if the quarternary C-atoms which are very often difficult to assign in polyene systems can be observed *via* a long-range correlation experiment [7]. In this case, the delays τ_1 and τ_2 are to be adjusted to give maximum polarization for the long-range C, H-couplings with simultaneous nulling of correlations for ¹*J*(C, H) [7].

After these applications of 2-D NMR to all-*trans*-retinal, we are convinced of the utility of 2-D NMR for the analysis of more complex polyene systems. When comparing the different experiments performed in the present work, the homo- and heteronuclear shift-correlated techniques might reveal to be more useful and more easy to interpret than the *J*-resolved techniques. The increase in time required in 2-D NMR appears generally more than offset by the additional information gained.

REFERENCES

- [1] G. Bodenhausen, R. Freeman & D. L. Turner, *J. Chem. Phys.* **65**, 839 (1976).
- [2] G. Bodenhausen, R. Freeman, R. Niedermeyer & D. L. Turner, *J. Magn. Reson.* **26**, 133 (1977).
- [3] R. Freeman & G. A. Morris, *Bull. Magn. Reson.* **1**, 5 (1979).
- [4] L. Müller, A. Kumar & R. R. Ernst, *J. Chem. Phys.* **63**, 5490 (1975).
- [5] W. P. Aue, E. Bartholdi & R. R. Ernst, *J. Chem. Phys.* **64**, 2229 (1976).
- [6] K. Nagayama, P. Bachmann, K. Wüthrich & R. R. Ernst, *J. Magn. Reson.* **31**, 133 (1978).
- [7] W. E. Hull, in 'Two Dimensional NMR', Bruker Brochure, Karlsruhe 1982.
- [8] G. Wider, R. Baumann, K. Nagayama, R. R. Ernst & K. Wüthrich, *J. Magn. Reson.* **42**, 73 (1981).
- [9] H. Kessler, W. Hehlein & R. Schuck, *J. Am. Chem. Soc.* **104**, 4534 (1982).
- [10] H. Kessler, W. Bernel, A. Friedrich, G. Krack & W. E. Hull, *J. Am. Chem. Soc.* **104**, 6297 (1982).
- [11] K. Nagayama & K. Wüthrich, *Eur. J. Biochem.* **114**, 365 (1981).
- [12] G. Wagner, A. Kumar & K. Wüthrich, *Eur. J. Biochem.* **114**, 375 (1981).
- [13] C. Bösch, A. Kumar, R. Baumann, R. R. Ernst & K. Wüthrich, *J. Magn. Reson.* **42**, 159 (1981).
- [14] D. L. Turner & R. Freeman, *J. Magn. Reson.* **29**, 587 (1978).
- [15] L. D. Hall & G. A. Morris, *Carbohydr. Res.* **82**, 175 (1980).
- [16] G. A. Morris & L. D. Hall, *J. Am. Chem. Soc.* **103**, 4703 (1981).
- [17] M. S. Broido & D. R. Kearns, *J. Magn. Reson.* **41**, 496 (1980).
- [18] P. P. Lankhorst, G. Wille, J. H. van Boom, C. Altona & C. A. G. Haasnoot, in 'Abstracts of the 6th European Experimental NMR Conference', Haute-Nendaz, Switzerland 1982, p. 90.
- [19] J. Lauterwein & C. Pattaroni, *Biochem. Biophys. Res. Commun.* **108**, 1300 (1982).
- [20] J. Lauterwein & J. M. Lhoste, in preparation.
- [21] G. Englert, *Helv. Chim. Acta* **58**, 2367 (1975).
- [22] G. D. Moss, *Pure Appl. Chem.* **51**, 507 (1979).
- [23] J. Wernly, M. Rey & J. Lauterwein, in 'Abstracts of the 6th European Experimental NMR Conference', Haute-Nendaz, Switzerland 1982, p. 67.
- [24] D. J. Patel, *Nature* **221**, 825 (1968).
- [25] B. Honig, B. Hudson, B. D. Sykes & M. Karplus, *Proc. Nat. Acad. Sci. USA* **68**, 1289 (1971).
- [26] R. Rowan, III, A. Warshel, B. D. Sykes & M. Karplus, *Biochemistry* **13**, 970 (1974).
- [27] R. Rowan, III & B. D. Sykes, *J. Am. Chem. Soc.* **96**, 7000 (1974).
- [28] R. S. Becker, S. Berger, D. K. Dalling, D. M. Grant & R. J. Pugmire, *J. Am. Chem. Soc.* **96**, 7008 (1974).
- [29] Y. Inoue, A. Takahashi, Y. Tokitô, R. Chûjô & Y. Miyoshi, *Org. Magn. Reson.* **6**, 487 (1974).
- [30] G. Bodenhausen, R. Freeman & D. L. Turner, *J. Magn. Reson.* **27**, 511 (1977).
- [31] K. Nagayama, A. Kumar, K. Wüthrich & R. R. Ernst, *J. Magn. Reson.* **40**, 321 (1980).
- [32] A. De Marco & K. Wüthrich, *J. Magn. Reson.* **24**, 201 (1976).
- [33] A. Bax & G. A. Morris, *J. Magn. Reson.* **42**, 501 (1981).
- [34] C. Pattaroni & J. Lauterwein, *Helv. Chim. Acta* **64**, 1969 (1981).
- [35] A. Kumar, *J. Magn. Reson.* **30**, 227 (1978).
- [36] G. Bodenhausen, R. Freeman, G. A. Morris & D. L. Turner, *J. Magn. Reson.* **31**, 785 (1978).
- [37] R. Baumann, G. Wider, R. R. Ernst & K. Wüthrich, *J. Magn. Reson.* **44**, 402 (1981).
- [38] W. Bremser, H. D. W. Hill & R. Freeman, *Messtechnik* **79**, 14 (1971).
- [39] K. Nagayama, K. Wüthrich & R. R. Ernst, *Biochem. Biophys. Res. Commun.* **90**, 305 (1979).
- [40] K. Nagayama, A. Kumar, K. Wüthrich & R. R. Ernst, *J. Magn. Reson.* **40**, 321 (1980).
- [41] R. Freeman, G. A. Morris & D. L. Turner, *J. Magn. Reson.* **26**, 373 (1977).
- [42] G. Bodenhausen, R. Freeman, G. A. Morris & D. L. Turner, *J. Magn. Reson.* **28**, 17 (1977).
- [43] J. B. Stothers, in 'Carbon-13 NMR Spectroscopy', Academic Press, London 1972, p. 355.
- [44] G. Englert, in 'Carotenoid Chemistry and Biochemistry', G. Britton and T. W. Goodwin, Eds., Pergamon, London 1981, p. 107.
- [45] D. L. Turner, *J. Magn. Reson.* **39**, 391 (1980).
- [46] D. M. Thomas, M. R. Bendall, D. T. Pegg, D. M. Doddrell & J. Field, *J. Magn. Reson.* **42**, 298 (1981).
- [47] A. Bax & R. Freeman, *J. Am. Chem. Soc.* **104**, 1099 (1982).
- [48] Y. Hanafusa, M. Toda, Y. Inoue & R. Chûjô, *Bull. Chem. Soc. Jpn.* **53**, 239 (1980).
- [49] G. A. Morris & L. D. Hall, *Can. J. Chem.* **60**, 2431 (1982).